16. E. Szathmáry, *J. Theor. Biol.* **159**, 99–109 (1992).
17. E. Szathmáry, J. Maynard Smith, *J. Theor. Biol.* **187**, 555–571 (1997).
18. C. M. Dobson, G. B. Ellison, A. F. Tuck, V. Vaida, *Proc. Natl. Acad. Sci. U.S.A.* **97**, 11864–11868 (2000).
19. E. V. Koonin, W. Martin, *Trends Genet.* **21**, 647–654 (2005).
20. A. Kanavarioti, P. A. Monnard, D. W. Deamer, *Astrobiology* **1**, 271–281 (2001).
21. T. Czárán, E. Szathmáry, in *The Geometry of Ecological Interactions: Simplifying Spatial Complexity,* U. Dieckmann, R. Law, J. A. J. Metz, Eds. (IIASA and Cambridge University Press, Cambridge, 2000), pp. 116–134.
22. P. Szabó, I. Scheuring, T. Czárán, E. Szathmáry, *Nature* **420**, 340–343 (2002).
23. P. L. Luisi, P. Walde, T. Oberholzer, *Curr. Op. Coll. Int. Sci.* **4**, 33–39 (1999).
24. M. T. Guo, A. Rotem, J. A. Heyman, D. A. Weitz, *Lab Chip* **12**, 2146–2155 (2012).
25. H. C. Guo, R. A. Collins, *EMBO J.* **14**, 368–376 (1995).
26. D. R. Mills, F. R. Kramer, S. Spiegelman, *Science* **180**, 916–927 (1973).
27. A. Traulsen, A. M. Sengupta, M. A. Nowak, *J. Theor. Biol.* **235**, 393–401 (2005).
28. B. Könnyu, T. Czárán, E. Szathmáry, *BMC Evol. Biol.* **8**, 267 (2008).
29. S. Ohno, *Evolution by Gene Duplication*. (Springer, New York, 1970).
30. J.-C. Baret *et al.*, *Lab Chip* **9**, 1850–1858 (2009).

**ACKNOWLEDGMENTS**

Comments by M. Santos and H. de Vladar are gratefully acknowledged. This work was supported by the European Union Seventh Framework Program (FP7/2007–2013) under grant agreements 225167 (eFlux) and 294332 (EvoEvo).

**SUPPLEMENTARY MATERIALS**

www.sciencemag.org/content/354/6317/1293/suppl/DC1
Materials and Methods
Supplementary Text
Figs. S1 to S12
Database S1
References (*31*–*42*)

17 May 2016; accepted 9 November 2016
10.1126/science.aag1582

SYNTHETIC BIOLOGY

# β-cell–mimetic designer cells provide closed-loop glycemic control

**Mingqi Xie,[1] Haifeng Ye,[2] Hui Wang,[1] Ghislaine Charpin-El Hamri,[3] Claude Lormeau,[1,4] Pratik Saxena,[1] Jörg Stelling,[1,4]* Martin Fussenegger[1,5]***

**Chronically deregulated blood-glucose concentrations in diabetes mellitus result from a loss of pancreatic insulin-producing β cells (type 1 diabetes, T1D) or from impaired insulin sensitivity of body cells and glucose-stimulated insulin release (type 2 diabetes, T2D). Here, we show that therapeutically applicable β-cell–mimetic designer cells can be established by minimal engineering of human cells. We achieved glucose responsiveness by a synthetic circuit that couples glycolysis-mediated calcium entry to an excitation-transcription system controlling therapeutic transgene expression. Implanted circuit-carrying cells corrected insulin deficiency and self-sufficiently abolished persistent hyperglycemia in T1D mice. Similarly, glucose-inducible glucagon-like peptide 1 transcription improved endogenous glucose-stimulated insulin release and glucose tolerance in T2D mice. These systems may enable a combination of diagnosis and treatment for diabetes mellitus therapy.**

Diabetes mellitus is a complex and progressive disease with a pathophysiology involving metabolic impairments that can lead to many clinical complications and currently affects more than 415 million people worldwide (*1*, *2*). Diabetic patients have a chronically elevated blood-glucose concentration, called hyperglycemia, that results from either a selective autoimmune destruction of pancreatic insulin-producing β cells (type 1 diabetes, T1D) or a progressive exhaustion of active β cells due to environmental factors that include a sedentary lifestyle, malnutrition, or obesity (type 2 diabetes, T2D) (*2*, *3*). Unless treated in time, sustained hyperglycemia can initiate pathologic cascades that result in more severe disorders such as cardiovascular diseases, renal failures, the metabolic syndrome, or hormone dysfunctions (*4*–*7*). Therefore, improved glycemic control by a therapeutic intervention that either enables tightly controlled insulin delivery or restores a patient's β-cell function will be important in diabetes treatment (*8*).

Because T1D patients suffer from complete insulin deficiency (*3*, *9*), treatment options focus on a disciplined or automated supply of exogenous insulin (*10*). For T2D therapy, there are more treatment options, owing to the progressive and multifactorial nature of this disease type (*1*, *2*). For example, incretin hormones [e.g., glucagon-like peptide 1 (GLP-1) analogs] improve glucose-stimulated insulin secretion of exhausting β cells (*11*). Recent studies capitalizing on engineered mammalian cells to produce insulinogenic proteins within a patient are gathering momentum because they promise effective drug production, delivery, and dosage (*12*). For example, the regeneration of glucose-responsive insulin-secreting β cells from stem cells (*9*, *13*) represents a breakthrough as transplantation of these ex vivo reprogrammed cells into T1D patients would restore their glucose-stimulated insulin expression. Alternatively, engineering of glucose-responsive insulin expression elements into extrapancreatic mammalian cell types (*14*) can protect against diabetic vulnerabilities such as autoimmune (re)targeting in T1D (*15*) and metabolic stress-induced β-cell apoptosis in T2D (*16*). Recently, synthetic biology–inspired rational circuit design has led to the engineering of immunoprotective implants, providing trigger-inducible insulin (*17*) or GLP-1 expression (*18*) with traceless and non-invasive signals. However, neither of these approaches provided closed-loop control of therapeutic dosage based on glucose sensing.

We engineered a glucose-inducible transcriptional system in an extrapancreatic human cell line that directly senses glycemia-relevant extracellular glucose concentrations and coordinates dose-dependent transcription of insulin and GLP-1. Glucose sensing was achieved by coupling a β-cell–mimetic cascade of glycolysis-mediated calcium entry (*19*) to a synthetic excitation-transcription coupling system (*20*) in human embryonic kidney 293 (HEK-293) cells. HEK-293 is widely used to study ion-channel activities and enables high-level production of antidiabetic proteins (*17*, *18*, *21*, *22*). We designed a HEK-293–based assay to evaluate the stimulus strength of membrane depolarization (Fig. 1A). When exposing different calcium-responsive promoters to 75 mM potassium chloride (KCl), the synthetic promoter $P_{NFAT2}$, containing nuclear factor of activated T cells (NFAT) repeats from the murine interleukin-4 (IL-4) promoter (*23*), was most responsive to chemically induced membrane depolarization (Fig. 1B). Cotransfection of a voltage-gated calcium channel such as $Ca_v1.2$ showed amplified excitation-transcription coupling and higher sensitivity (Fig. 1C). Five tandem $NFAT_{IL4}$-repeats 5′ of a minimal promoter [pMX57, $P_{NFAT3}$-SEAP-pA; $P_{NFAT3}$, $(NFAT_{IL4})_5$-$P_{min}$] showed optimal induction ratios between resting and depolarized membrane potentials (Fig. 1D) and could distinguish between signals generated by voltage-gated calcium channels of different activation thresholds (Fig. 1E).

To evaluate the effects of each β-cell–derived component for sensing glucose [the glucose transporter 2 (GLUT2), glucokinase (GCK), ATP-sensitive potassium channel ($K_{ATP}$), and voltage-gated calcium channel ($Ca_v1.3$)] with the pMX57-based depolarization assay, we used a combinatorial screening approach (Fig. 2, A and B). Expression of $K_{ATP}$ did not improve glucose sensing; overexpression of GLUT2 increased glucose-induced

[1]Department of Biosystems Science and Engineering, ETH Zurich, Mattenstrasse 26, CH-4058 Basel, Switzerland. [2]Shanghai Key Laboratory of Regulatory Biology, Institute of Biomedical Sciences and School of Life Sciences, East China Normal University, Dongchuan Road 500, 200241 Shanghai, China. [3]Institut Universitaire de Technologie, IUT, Département Génie Biologique, F-69622 Villeurbanne Cedex, France. [4]SIB–Swiss Institute of Bioinformatics, ETH Zurich, Mattenstrasse 26, CH-4058 Basel, Switzerland. [5]University of Basel, Faculty of Science, Mattenstrasse 26, CH-4058 Basel, Switzerland.
***Corresponding author. Email: fussenegger@bsse.ethz.ch (M.F.); joerg.stelling@bsse.ethz.ch (J.S.)**

calcium-dependent transcription; and GCK overexpression appeared to cause toxic effects at higher extracellular glucose concentrations (Fig. 2B). Indeed, semiquantitative transcriptional profiling confirmed that GLUT1 (*24*) as well as $K_{ATP}$ are endogenously expressed in HEK-293 cells (fig. S1A), and most mammalian cells express at least one hexokinase isoform (*25*). Therefore, ectopic expression of the $Ca_v1.3$ channel was sufficient to confer glucose sensitivity to HEK-293 cells (Fig. 2B). In contrast, putative glucose sensors such as the T1R2/T1R3 sweet taste receptors (*26*) failed to respond to glucose concentrations relevant for glycemic control (fig. S1B). Therefore, $Ca_v1.3$ represents the missing component needed to reconstitute an intact, physiologically relevant glucose-sensing cascade in HEK-293 cells (Fig. 2A) and to establish mimetic β-cell function in nonpancreatic human cells.

To quantitatively analyze the β-cell–derived glucose-sensing cascade, ensure consistency in the design steps, and predict circuit operation in vivo, we developed a dynamic mathematical model (fig. S6 and supplementary methods). This ordinary differential equation (ODE) model covers the components shown in Fig. 2, a detailed representation of the cell's electrophysiology (fig. S7), and a previously developed representation of in vivo glucose-insulin regulation (*21*). We parametrized the model with experimental data across conditions and experimental assays (supplementary methods) to establish a single, quantitative representation of the system. The model reproduced, among others, the potassium (Fig. 1E) and glucose (Fig. 2B) dose-response curves; it was used for quantitative circuit characterization and essential predictions of in vivo behaviors.

To test the substrate specificity of the $Ca_v1.3$/$P_{NFAT3}$-constituted glucose-sensing system, we cultured $Ca_v1.3$/pMX57-transgenic HEK-293 cells in media containing osmotic controls (fig. S2A), common dietary sugars (fig. S2B), or other nutrients (fig. S2C). D-Glucose was the only substrate that activated human placental secreted alkaline phosphatase (SEAP) expression from the synthetic excitation-transcription coupling system at physiologically relevant concentrations. Additionally, the glucose-sensing system was insensitive to inflammatory cytokines inducing NFAT signaling pathways (*27*) (fig. S2, D and E). Capitalizing on the tight induction kinetics of the $P_{NFAT3}$-regulated gene expression system (fig. S3) and on the system's strict $Ca_v1.3$-dependent activation (fig. S4), we constructed a stable human HEK-$293_{NFAT\text{-}SEAP1}$ cell line transgenic for $P_{NFAT3}$-driven SEAP expression (fig. S5). Ectopic expression of the $Ca_v1.3$ channel in HEK-$293_{NFAT\text{-}SEAP1}$ resulted in improved induction ratios between low and high extracellular glucose concentrations (Fig. 2C; ~4.6 fold-induction from 5 to 25 mM glucose) compared to the transient configuration (Fig. 2B; ~2.6 fold-induction). Glucose-stimulated induction of $Ca_v1.3$-transgenic HEK-$293_{NFAT\text{-}SEAP1}$ cells was significant within 24 hours and reached maximal SEAP levels after cultivation in high-glucose medium for 48 hours (Fig. 2D). Additionally, SEAP expression could be switched to dose-dependent regulation even after maintaining the $Ca_v1.3$-transgenic HEK-$293_{NFAT\text{-}SEAP1}$ cells in low-glucose conditions (2 mM) for different

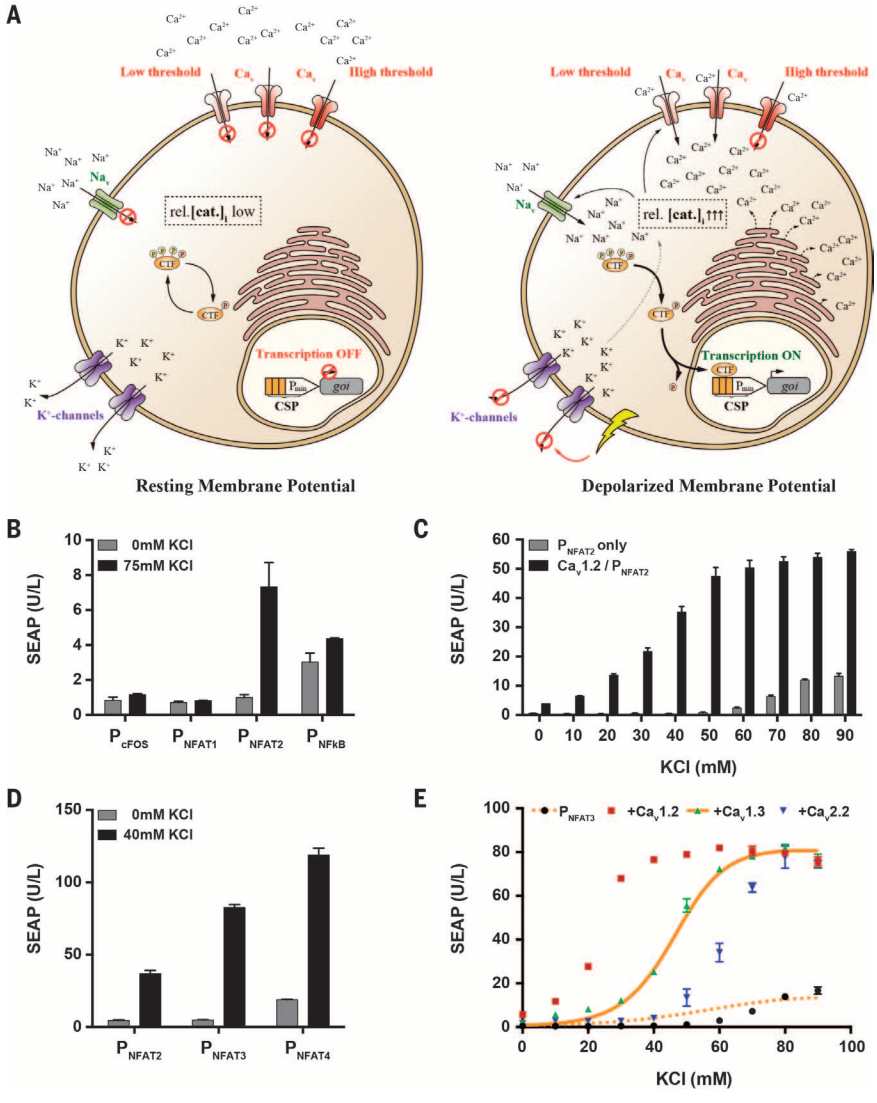


**Fig. 1. Engineering of an excitation-transcription coupling system.** (**A**) Diagram of the synthetic excitation-transcription coupling system. At resting membrane potentials, basal ion currents keep the relative concentration of intracellular cations (rel.[cat.]$_i$) low, the plasma membrane hyperpolarized, and calcium-specific promoters (CSPs) repressed. Blocking of $K^+$ channels or triggered cation entry increases rel.[cat.]i; depolarizes the membrane potential, which is amplified by the opening of threshold-dependent voltage-gated sodium ($Na_v$) or calcium ($Ca_v$) channels; and promotes nuclear translocation of calcium-responsive transcription factors to induce CSP-driven gene expression. (**B** to **E**) Functional tests: cells were depolarized with KCl, and SEAP levels were profiled after 48 hours. (B) CSPs activated by chemically induced membrane depolarization: HEK-293 transfected with pMX53 ($P_{cFOS}$-SEAP-pA), pHY30 ($P_{NFAT1}$-SEAP-pA), pMX56 ($P_{NFAT2}$-SEAP-pA), or pKR32 ($P_{NFκB}$-SEAP-pA). (C) $Ca_v1.2$-amplified excitation-transcription coupling: HEK-293 (co)transfected with pMX56 ($P_{NFAT2}$-SEAP-pA) and $Ca_v1.2$. (D) CSP optimization: HEK-293 cotransfected with $Ca_v1.2$ and CSP-driven SEAP expression vectors (pMX56, $P_{NFAT2}$-SEAP-pA; pMX57, $P_{NFAT3}$-SEAP-pA; pMX58, $P_{NFAT4}$-SEAP-pA). (E) Activation threshold–dependent excitation-transcription coupling: HEK-293 cotransfected with pMX57 and either $Ca_v1.2$, $Ca_v1.3$, or $Ca_v2.2$. Experimental (symbols) and simulation data (lines) are combined. All experimental data presented are mean ± SD, $n \geq 5$ independent experiments.

periods of time (fig. S8A), and an independent time-course experiment showing glucose-mediated sensitization, as well as starvation-mediated desensitization, confirmed the reversibility of the synthetic excitation-transcription coupling system (fig. S8B). The mathematical model reproduced this behavior quantitatively (Fig. 2, C and D, and figs. S8B and S9), and independent predictions for varying $Ca_v1.3$ dosages agreed well with experiments (Fig. 2), emphasizing the model's consistency across constructs and conditions.

To test the potential of the glucose-induced excitation-transcription coupling system for diabetes treatment, we implanted $Ca_v1.3$-transgenic HEK-293$_{NFAT\text{-}SEAP1}$ cells microencapsulated in clinically validated alginate beads (*28*) intraperitoneally into mice. In vivo, our implanted transcriptional regulation system operated in a dose- and $Ca_v1.3$-dependent manner, as recapitulated by the same in vitro dynamic model coupled to a mathematical representation of mouse physiology (fig. S10). Notably, the system translated the characteristic average fasting glycemia values of wild-type as well as T1D- and T2D-diabetic mouse models into correspondingly expressed SEAP levels in the serum (Fig. 3A and fig. S11).

State-of-the-art treatment options for diabetes mellitus are either long-acting drugs, such as stabilized GLP-1 variants that allow a decrease in the administration frequency to weekly periods (T2D) (*1*, *29*), or portable electronic pump systems that self-sufficiently inject rapid-acting insulin analogs according to the patient's instantaneous glycemia (T1D) (*10*, *30*). To test whether the GLP-1 expression levels achieved by the glucose-inducible excitation-transcription coupling system were compatible with T2D treatment, we cotransfected HEK-293 cells with $Ca_v1.3$ and the short human GLP-1 (shGLP1) variant (*18*) (pMX115; $P_{NFAT5}$-shGLP1-pA), which enabled exclusive GLP-1 expression under hyperglycemic conditions (fig. S12A). Implanting $5 \times 10^6$ microencapsulated $Ca_v1.3$/pMX115-transgenic HEK-293 cells into T2D mice resulted in self-sufficient GLP-1 expression (Fig. 3B) and substantially improved glucose-stimulated insulin secretion (Fig. 3C) and glucose tolerance (Fig. 3D). Similarly, cotransfection of $Ca_v1.3$ with an insulin expression vector (pMX100; $P_{NFAT5}$-mINS-pA) (*21*) provided hyperglycemia-triggered insulin expression (fig. S12B). In agreement between experiments and model, self-sufficient insulin expression from $Ca_v1.3$/pMX100-transgenic implants not only restored the typical insulin deficiency in a T1D mouse model (fig. S13A) but also corrected the animals' persistent hyperglycemia within 2 to 3 days (fig. S13B). Notably, hypoglycemic side effects resulting from basal or excessive insulin expression at normoglycemic levels that are often observed in classical insulin monotherapies (*10*) or with immature β cells (*31*) were not detected (fig. S13, A and B).

We conducted extensive simulation studies to systematically assess potential side effects associated with the robustness of hyperglycemia-triggered insulin expression when the patient's physiological state is unknown or changing. The model predicted that an implant would improve glucose tolerance (fig. S13, C and D) and might provide self-sufficient inactivation during parallel insulin therapies (fig. S13E) and/or reactivation in cases of recurrent β-cell loss (fig. S13F). Indeed, implantation of microencapsulated HEK-β cells (Fig. 4A) stably transgenic for reversible glucose-stimulated insulin secretion (figs. S14 and S15) restored glucose (Fig. 4B) and blood insulin homeostasis (Fig. 4C) in T1D mice as predicted by the mathematical model (fig. S13). Glucose homeostasis of treated T1D mice was robust during the entire 3-week study (Fig. 4B), and treated animals challenged by glucose tolerance tests (Fig. 4D) to simulate meal responses did not suffer from glycemic excursions during the HEK-β–mediated restoration of normoglycemia (Fig. 4B). In contrast, T1D mice receiving negative-control implants ($Ca_V1.3$/pMX115-transgenic HEK-293 cells) remained hyperglycemic and did not survive the first glucose tolerance test at day 7 (Fig. 4, B and D).



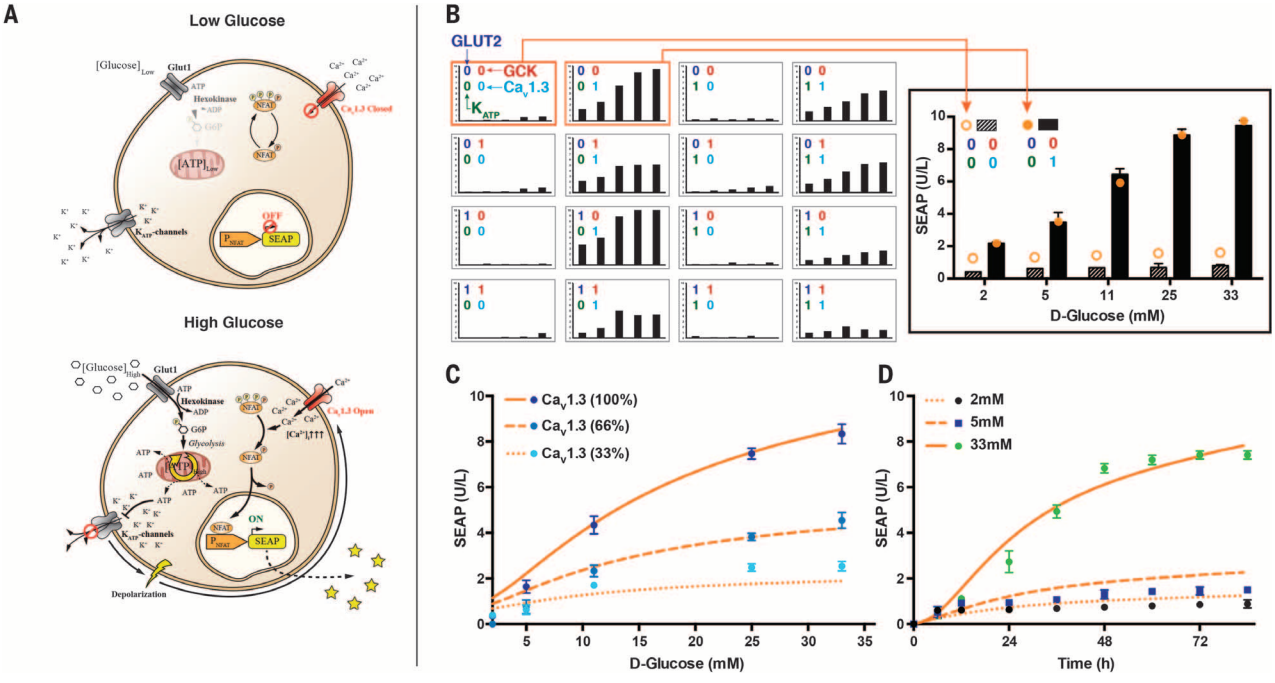


**Fig. 2. Glucose sensing by extrapancreatic human cells.** (**A**) Diagram of glucose sensing in engineered HEK-293 cells. Low extracellular glucose does not lead to membrane depolarization–based activation of voltage-gated $Ca_v1.3$ channels. High extracellular glucose results in glucose uptake, increased adenosine 5′-triphosphate (ATP) production, closure of ATP-sensitive potassium channels ($K_{ATP}$), $Ca_v1.3$-mediated $Ca^{2+}$ influx, and calcineurin-dependent SEAP induction by synthetic $P_{NFAT}$ promoters. (**B**) Combinatorial analysis of glucose-sensing components in extrapancreatic human cells. HEK-293 cotransfected with pMX57 ($P_{NFAT3}$-SEAP-pA) and either constitutive hGLUT2, GCK, $K_{ATP}$, $Ca_v1.3$ expression vectors (1), or pcDNA3.1(+) (0) were cultivated at the indicated glucose concentrations, and SEAP levels were profiled after 48 hours. (**C**) $Ca_v1.3$-dependent glucose sensing. HEK-293$_{NFAT\text{-}SEAP1}$ transfected with different amounts of $Ca_v1.3$ (100%: 2000 ng) were cultivated at different glucose concentrations and SEAP levels were profiled after 48 hours. (**D**) SEAP expression kinetics. $Ca_v1.3$-transgenic HEK-293$_{NFAT\text{-}SEAP1}$ were cultivated at the indicated glucose concentrations, and SEAP levels were profiled at 12-hour intervals. Orange lines and dots show corresponding simulations. Data presented are mean ± SD, $n \geq 5$ independent experiments.

β cells modulate insulin release not only in response to glucose but also by the action of glucoincretins such as GLP-1 (*29*). We therefore engineered HEK-293 for HEK-β componentry, as well as for constitutive expression of the GLP-1 receptor (GLP1R) and $P_{CRE}$-driven insulin expression (Fig. 4E). The resulting HEK-$β_{GLP}$ showed insulin secretion dynamics (fig. S16) similar to that of HEK-β, but was also sensitive to the animals' food intake (Fig. 4F). Although HEK-$β_{GLP}$ was similar to HEK-β in attenuating glycemic excursions in oral glucose tolerance tests (Fig. 4G), glucose homeostasis was less efficiently restored in T1D mice compared to HEK-β (Fig. 4H). This finding was confirmed by model simulations (fig. S17) and established HEK-β as the prime β-cell–mimetic design.

In a comparative analysis of reversible glucose-stimulated insulin secretion by HEK-β, the pancreatic β-cell line 1.1E7 (*32*), and human islets over 3 weeks, HEK-β showed higher insulin secretion capacity than 1.1E7 and human islets in vitro (fig. S15C). In T1D mice, microencapsulated HEK-β and 1.1E7 were equally efficient in establishing postprandial glucose metabolism (Fig. 4G), but HEK-β restored glucose homeostasis more efficiently than 1.1E7 after 2 weeks and reached fasting glycemia levels of wild-type mice over the 3-week period (Fig. 4B). With human islets, postprandial glucose metabolism could only be restored in two out of four T1D mice (fig. S18), which confirms performance variations of encapsulated human islets (*28*). However, in these two T1D mice, the human islets provided glucose tolerance similar to that of HEK-β (Fig. 4D).

State-of-the-art strategies for cell-based treatment of diabetes include a variety of approaches such as islet transplantation (*33*), differentiation of β-like cells from pluripotent precursor cells using culture additives (*9*, *13*) or genetic lineage-control networks (*34*), and designer cells engineered for trigger-controlled insulin or GLP-1 secretion (*17*, *18*). β-cell mimetics coordinate precise sensing of blood-glucose concentrations and insulin production in a dose-dependent, reversible, and closed-loop manner. The quest for biological glucose sensors has resulted in the design of several biosensors, but they were either not sufficiently sensitive (*26*) or quantified glucose indirectly (*21*). By contrast, our strategy to evaluate the components managing glucose sensing in native β cells has revealed $Ca_V1.3$ as the single most important component that programs extrapancreatic human cells such as HEK-293 to profile physiological blood-glucose concentrations in a precise, reversible, and dynamic fashion. Coupling of $Ca_V1.3$-based glucose sensing to insulin production and secretion resulted in the β-cell–mimetic HEK-β that provided increased 3-week insulin secretion profiles compared to the pancreatic cell line 1.1E7 and human islets in vitro. Control of postprandial glucose metabolism was similar between HEK-β and 1.1E7, but only HEK-β reached the blood glucose concentrations of healthy mice. Because the different insulin-release dynamics of HEK-β, 1.1E7, and human islets in vitro had no substantial impact on postprandial glucose metabolism, the differences in the secretion modality—constitutive for HEK-β, vesicular for 1.1E7 and human islets—may not be as relevant in response to meals as generally thought. This is supported by our model simulations and by the latest generation of basal insulin analogs such as insulin degludec (Tresiba, Novo Nordisk), which provides autonomous glucose control for up to 42 hours without the need to synchronize its administration with meals (*35*).

Human islets seem to be the optimal choice for cell-based diabetes therapies because the β cells are embedded in an organ structure, providing optimal support for glycemic control (*31*). However, human islets are in chronically short supply (*34*) and difficult to maintain in culture, and as a result of quality variations of available donor batches, treatment success remains unpredictable (*31*). Although immortalized β-cell lines have been developed to overcome the cultivation and quality issues of human islets, none of the available β-cell lines shows the performance level of glucose-induced insulin release required for successful diabetes therapy (*32*). Therefore, recent strategies for cell-based diabetes treatment focus on differentiation of (induced pluripotent) stem cells into β-like cells using mixtures of chemicals and growth factors (*9*, *13*) or rational programming by synthetic lineage-control networks (*34*). Although β-like cells produced from in vitro–differentiated pancreatic progenitor cells may have a promising future (clinical trial NCT02239354), available differentiation protocols are complex, expensive, and likely incompatible with large-scale bioprocessing. Additionally, in vitro–differentiated β-like cells require considerable time to mature into β cells after implantation, which may limit the life span of the implant before inactivation by fibrosis (*36*). β-cell–mimetic designer cells such as HEK-β could provide an attractive alternative: (i) They use glucose-sensor components evolved in native β cells (*19*), (ii) take advantage of robust parental cell lines with a track record in biopharmaceutical manufacturing (*37*), and (iii) show glucose-induced insulin release performance comparable to that of β-cell lines and

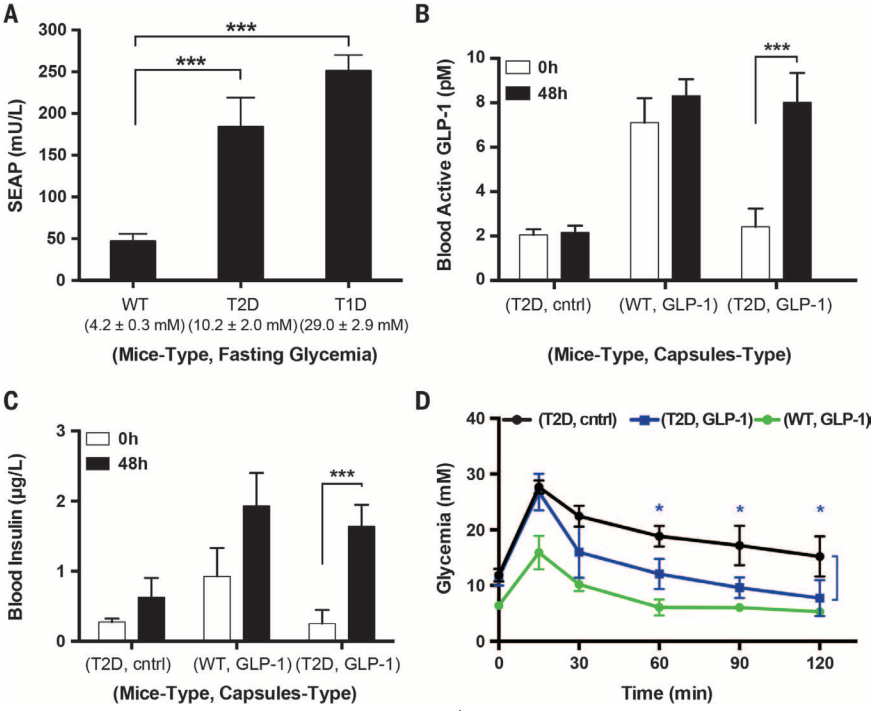


**Fig. 3. $Ca_v1.3$-dependent glucose sensing and antidiabetic treatment potential in diabetic mice.** (**A**) Dose-dependent glycemia-induced SEAP expression in diabetic mice. Microencapsulated $Ca_v1.3$-transfected HEK-$293_{NFAT\text{-}SEAP1}$ ($1 \times 10^4$; 500 cells per capsule) were implanted into mice suffering from type 1 (T1D) or type 2 (T2D) diabetes, and blood SEAP levels were quantified after 48 hours. (**B** and **C**) Self-sufficient GLP-1 expression in wild-type (WT) and T2D mice. Microencapsulated HEK-293 cells cotransfected with $Ca_v1.3$ and pMX115 ($P_{NFAT5}$-shGLP1-pA) ($1 \times 10^4$; 500 cells per capsule) were implanted into WT or T2D mice, and blood GLP-1 (B) as well as insulin (C) concentrations were quantified after 48 hours. Microencapsulated $Ca_v1.3$-transgenic HEK-$293_{NFAT\text{-}SEAP1}$ cells were used as a negative control (cntrl). (**D**) Intraperitoneal glucose tolerance test of WT and T2D mice. Treatment groups shown in (B) and (C) received intraperitoneal glucose injections (2 g per kilogram of body weight) 48 hours after implantation, and glycemic profiles of each animal were tracked every 30 min. Data are mean ± SEM; analysis was by two-tailed *t* test ($n$ = 8 mice). $^*P < 0.05$, $^{***}P < 0.001$ versus control.

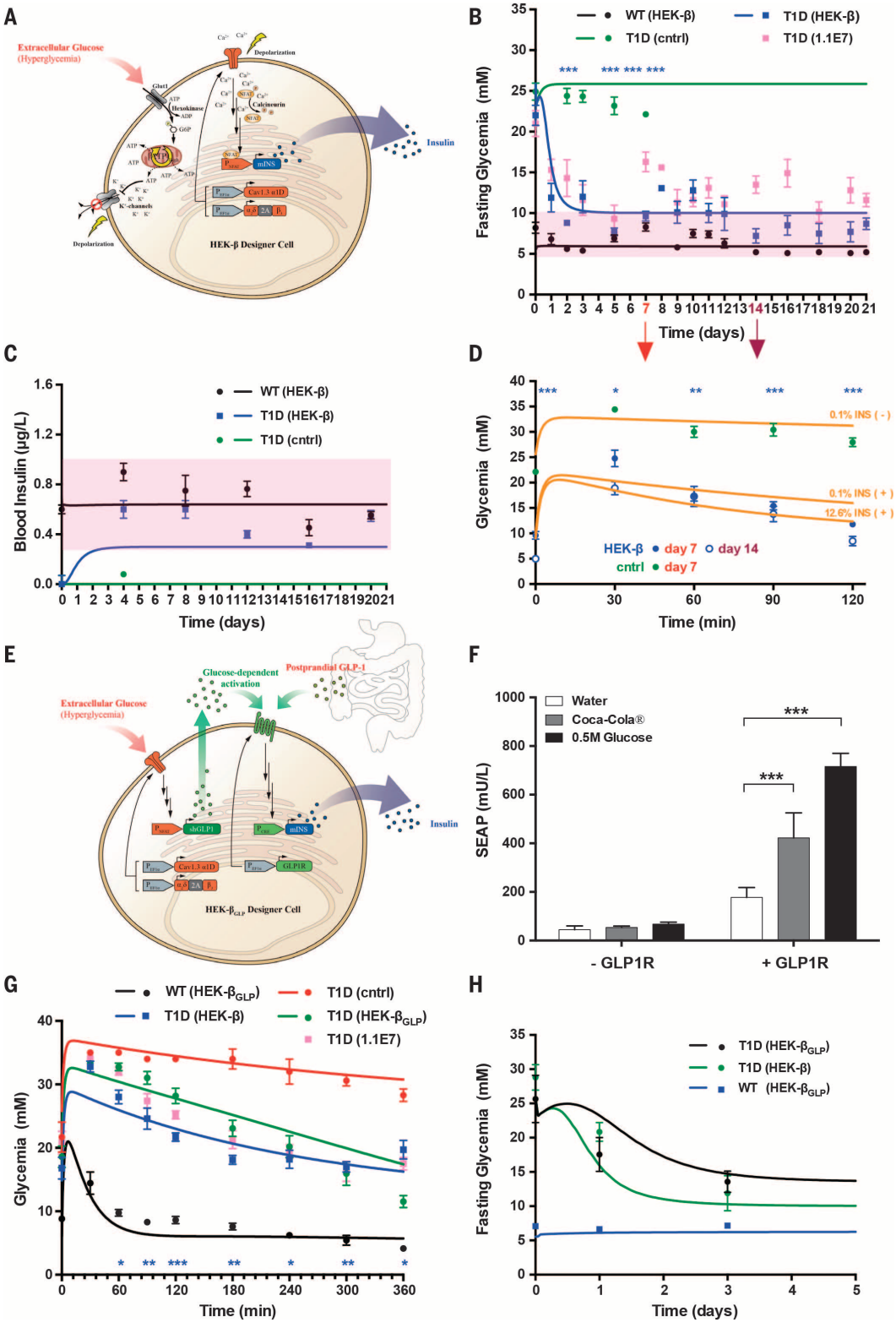


**Fig. 4. Treatment potential of β-cell–mimetic designer cells in T1D mice.** (**A**) Diagram of HEK-β. Extracellular D-glucose triggers glycolysis-dependent membrane depolarization, which activates the voltage-gated calcium channel $Ca_V1.3$, resulting in $Ca^{2+}$ influx, induction of the calmodulin-calcineurin signaling cascade, and $P_{NFAT}$-mediated induction of insulin secretion. (**B**) Self-sufficient glycemic control in WT and T1D mice. Microencapsulated HEK-β or 1.1E7 cells (500 cells per capsule) were implanted into WT and T1D mice ($1 \times 10^4$ capsules per mouse), and fasting glycemia was recorded for 3 weeks. T1D mice treated with negative-control implants ($Ca_V1.3$/pMX115-transgenic HEK-293; cntrl) did not survive the first glucose tolerance test on day 7 (D). (**C**) Self-sufficient insulin expression in WT and T1D mice. Postprandial blood insulin concentrations of treatment groups shown in (B) were profiled for up to 3 weeks. Curves of matching colors [(B) and (C)] represent corresponding model-based predictions. Physiological blood glucose and insulin concentrations are indicated by a red background. (**D**) Intraperitoneal glucose tolerance tests in T1D mice. On days 7 and 14 (arrows), treatment groups shown in (B) and (C) received intraperitoneal glucose injections (2 g/kg), and glycemic profiles of each animal were tracked every 30 min. Orange lines represent model-based predictions with 0.1 to 12.6% residual insulin production treated with (+) or without (–) HEK-β implants (fig. S13C). (**E**) Diagram of HEK-$β_{GLP}$. Glucose triggers dose-dependent $P_{NFAT}$-driven expression of glucagon-like peptide 1 (shGLP1) for autocrine activation of ectopically expressed GLP-1 receptor (GLP1R), leading to $P_{CRE}$-driven insulin secretion. In vivo, insulin expression by HEK-$β_{GLP}$ cells may also be triggered following postprandial GLP-1 release by intestinal cells. (**F**) Response of β-cell–mimetic implants to meals. WT mice were implanted with $5 \times 10^6$ microencapsulated $Ca_V1.3$/pMX57-transgenic HEK-293 cells (-GLP1R) or $Ca_V1.3$/pMX61/pMX258-transgenic $HEK_{GLP1R}$ cells (+GLP1R) and received oral doses of 200 µl of $H_2O$, Coca-Cola, or sugared water (0.5 M glucose). Resulting blood SEAP levels were quantified after 48 hours. (**G**) Oral glucose tolerance test of WT and T1D mice. Mice received $5 \times 10^6$ microencapsulated HEK-β, 1.1E7 or HEK-$β_{GLP}$ or negative-control implants (cntrl; $Ca_V1.3$/pMX115-transgenic HEK-293). After oral administration of sugared water (2 g/kg glucose in $H_2O$), glycemic excursions were recorded for 6 hours. Curves of matching colors represent corresponding model simulations. (**H**) Self-sufficient glycemic control by implanted HEK-β and HEK-$β_{GLP}$. Microencapsulated HEK-β or HEK-$β_{GLP}$ cells ($5 \times 10^6$) were implanted into WT or T1D mice ($1 \times 10^4$ capsules per mouse), and fasting glycemia was recorded for 3 days. Curves of matching colors represent corresponding model simulations. Data are mean ± SEM, statistics by two-tailed *t* test ($n = 8$ mice). *$P < 0.05$, **$P < 0.01$, ***$P < 0.001$ HEK-β versus control.

human islets. Additionally, rational programming of designer cells enables (iv) straightforward fine-tuning of performance parameters and provides (v) flexibility to couple glucose sensing to the production of other therapeutic proteins such as GLP-1 required for T2D therapy (*1*, *29*).

## REFERENCES AND NOTES


1. S. Cornell, *Ther. Clin. Risk Manag.* **11**, 621–632 (2015).
2. J. Tuomilehto, S. Bahijri, *Nat. Rev. Endocrinol.* **12**, 127–128 (2016).
3. K. S. Polonsky, *N. Engl. J. Med.* **367**, 1332–1340 (2012).
4. S. J. Cleland, *Nat. Rev. Endocrinol.* **8**, 476–485 (2012).
5. G. I. Shulman, *N. Engl. J. Med.* **371**, 1131–1141 (2014).
6. S. M. Grundy, *Nat. Rev. Drug Discov.* **5**, 295–309 (2006).
7. P. M. Rao, D. M. Kelly, T. H. Jones, *Nat. Rev. Endocrinol.* **9**, 479–493 (2013).
8. J. E. Bruin *et al.*, *Stem Cell Rep.* **4**, 605–620 (2015).
9. A. Rezania *et al.*, *Nat. Biotechnol.* **32**, 1121–1133 (2014).
10. J. C. Pickup, *N. Engl. J. Med.* **366**, 1616–1624 (2012).
11. D. J. Drucker, M. A. Nauck, *Lancet* **368**, 1696–1705 (2006).
12. G. M. Church, M. B. Elowitz, C. D. Smolke, C. A. Voigt, R. Weiss, *Nat. Rev. Mol. Cell Biol.* **15**, 289–294 (2014).
13. F. W. Pagliuca *et al.*, *Cell* **159**, 428–439 (2014).
14. B. E. Tuch *et al.*, *Gene Ther.* **10**, 490–503 (2003).
15. C. Aguayo-Mazzucato, S. Bonner-Weir, *Nat. Rev. Endocrinol.* **6**, 139–148 (2010).
16. L. Marzban *et al.*, *Diabetes* **55**, 2192–2201 (2006).
17. S. A. Stanley *et al.*, *Science* **336**, 604–608 (2012).
18. H. Ye, M. Daoud-El Baba, R. W. Peng, M. Fussenegger, *Science* **332**, 1565–1568 (2011).
19. F. M. Ashcroft, P. Rorsman, *Nat. Rev. Endocrinol.* **9**, 660–669 (2013).
20. M. D'Arco, A. C. Dolphin, *Sci. Signal.* **5**, pe34 (2012).
21. D. Ausländer *et al.*, *Mol. Cell* **55**, 397–408 (2014).
22. H. Ye *et al.*, *Proc. Natl. Acad. Sci. U.S.A.* **110**, 141–146 (2013).
23. J. W. Rooney, M. R. Hodge, P. G. McCaffrey, A. Rao, L. H. Glimcher, *EMBO J.* **13**, 625–633 (1994).
24. M. Elsner, M. Tiedge, B. Guldbakke, R. Munday, S. Lenzen, *Diabetologia* **45**, 1542–1549 (2002).
25. R. B. Robey, N. Hay, *Oncogene* **25**, 4683–4696 (2006).
26. H. J. Jang *et al.*, *Proc. Natl. Acad. Sci. U.S.A.* **104**, 15069–15074 (2007).
27. F. Macian, *Nat. Rev. Immunol.* **5**, 472–484 (2005).
28. A. J. Vegas *et al.*, *Nat. Med.* **22**, 306–311 (2016).
29. G. G. Holz 4th, W. M. Kühtreiber, J. F. Habener, *Nature* **361**, 362–365 (1993).
30. S. J. Russell *et al.*, *N. Engl. J. Med.* **371**, 313–325 (2014).
31. T. J. Kieffer, *Cell Stem Cell* **18**, 699–702 (2016).
32. J. T. McCluskey *et al.*, *J. Biol. Chem.* **286**, 21982–21992 (2011).
33. D. W. Scharp, P. Marchetti, *Adv. Drug Deliv. Rev.* **67-68**, 35–73 (2014).
34. P. Saxena *et al.*, *Nat. Commun.* **7**, 11247 (2016).
35. A. N. Zaykov, J. P. Mayer, R. D. DiMarchi, *Nat. Rev. Drug Discov.* **15**, 425–439 (2016).
36. M. Kastellorizios, N. Tipnis, D. J. Burgess, *Adv. Exp. Med. Biol.* **865**, 93–108 (2015).
37. F. M. Wurm, *Nat. Biotechnol.* **22**, 1393–1398 (2004).


## ACKNOWLEDGMENTS

We thank V. Haellman and H. Zulewski for critical comments on the manuscript. This work was supported by a European Research Council advanced grant (ProNet no. 321381) and in part by the Natural Science Foundation of China (no. 31522017) and the National Centre of Competence in Research Molecular Systems Engineering. All data supporting the findings of this study are presented in the main paper and supplementary materials. Plasmids are available from M.F. on request. M.X. and M.F. are inventors on a patent application filed by the ETH Zurich on the β-cell mimetic designer cells (application nos. EP16180000.8 and EP16200258.8). M.X., H.Y., H.W., P.S. and G.C. conducted the experiments; C.L., M.X., and J.S. developed the mathematical model; M.X., C.L., J.S., and M.F. designed the experiments and wrote the manuscript.

## SUPPLEMENTARY MATERIALS

www.sciencemag.org/content/354/6317/1296/suppl/DC1
Materials and Methods
Supplementary Text
Figs. S1 to S18
Tables S1 to S12
References (*38*–*62*)

4 February 2016; accepted 10 November 2016
10.1126/science.aaf4006

VIRAL EVOLUTION

# Ecological speciation of bacteriophage lambda in allopatry and sympatry

**Justin R. Meyer,[1]* Devin T. Dobias,[2,3] Sarah J. Medina,[1] Lisa Servilio,[1] Animesh Gupta,[4] Richard E. Lenski[5]**

**Understanding the conditions that allow speciation to occur is difficult because most research has focused on either long-lived organisms or asexual microorganisms. We propagated bacteriophage λ, a virus with rapid generations and frequent recombination, on two *Escherichia coli* host genotypes that expressed either the LamB or OmpF receptor. When supplied with either single host (allopatry), phage λ improved its binding to the available receptor while losing its ability to use the alternative. When evolving on both hosts together (sympatry), the viruses split into two lineages with divergent receptor preferences. Although the level of divergence varied among replicates, some lineages evolved reproductive isolation via genetic incompatibilities. This outcome indicates that, under suitable conditions, allopatric and sympatric speciation can occur with similar ease.**

Studies of extant and extinct species provide evidence that biological evolution can promote diversification rather than mere replacement of one form by another (*1*). Moreover, asexual microbes frequently diversify when cultured in the laboratory (*2*), even in simple conditions that would seem to favor homogeneity (*3*). Sympatric diversification in sexual populations has long been thought to be difficult because constant recombination prevents an interbreeding population from splitting into genetically distinct lineages that occupy different ecological niches (*4*, *5*). However, putative examples of sympatric speciation have advanced the argument that speciation in a recombining population may occur under certain circumstances (*6*, *7*), although other studies have disputed these claims (*8*). This debate is important because the process of speciation is fundamental to biological evolution.

To shed light on this question, we conducted evolution experiments with viruses to examine the effect of recombination on their divergence into distinct ecological niches. We studied a virulent (i.e., strictly lytic) derivative of phage λ, which infects *Escherichia coli*. Most λ can use only a single outer-membrane protein, LamB, as a receptor, but the strain we studied, EvoC, can also exploit a second receptor, OmpF (*9*). The ability to use OmpF arose via five point mutations in the host-recognition gene, *J*. To examine λ diversification, we propagated virus populations on one or both of two strains of *E. coli* that differ only in whether they possess the *lamB* or *ompF* genes, which encode LamB and OmpF, respectively (*10*). Phages tend to exploit specific receptors (*11*), leading us to predict that populations of the generalist phage EvoC would evolve toward increased receptor specificity. Whether or not two receptor specialists evolved, however, would likely also depend on the effects of recombination. When two or more λ viruses infect the same cell, their genomes can recombine (*12*).

We use λ as a model for analyzing the mechanisms of speciation. Viruses are diverse (*13*), and their rates and mechanisms of speciation will depend on their life histories, just as the rates and mechanisms vary in plants and animals. However, some salient features of speciation are shared, even across such distant taxa. For example, viruses that infect the same species and cell types are thought to have evolved mechanisms to limit recombination, including divergences in nucleotide composition and RNA structure that are analogous to prezygotic barriers in plants and animals (*14*–*16*). One feature of our system that might promote sympatric speciation is the connection between the viruses' ecological niches (i.e., host cells) and where genetic exchange occurs. Specialists that use the same receptor will naturally tend to recombine because they are more likely to infect the same host. Therefore, reproductive isolation can evolve as a by-product of ecological divergence, without requiring other mutations that govern recombination. Such dual-effect mutations have been described in other systems and are important because their simultaneous effects on ecological niches and mating

[1]Division of Biology, University of California San Diego (UCSD), La Jolla, CA 92093, USA. [2]Department of Biology, Washington University, St. Louis, MO 63130, USA. [3]Department of Biology, Loyola University Chicago, 1032 West Sheridan Road, Chicago, IL 60660, USA. [4]Department of Physics, UCSD, La Jolla, CA 92093, USA. [5]Department of Microbiology and Molecular Genetics and BEACON Center for the Study of Evolution in Action, Michigan State University, East Lansing, MI 48824, USA.
*Corresponding author. Email: justin.raymond.meyer@gmail.com

Editor's Summary

**Engineering cells to regulate glucose**

Diabetes mellitus affects hundreds of millions of people worldwide. Blood glucose levels are chronically deregulated in diabetics, and this can lead to many serious disorders, including cardiovascular disease and renal failure. Xie *et al.* engineered a synthetic circuit into human cells that can sense the glucose concentration and respond to correct deregulation. Implants containing designer cells improved glucose regulation in diabetic mice.

*Science*, this issue p. 1296